Journal of Soils and Sediments
https://doi.org/10.1007/s11368-021-02946-7

SEDIMENT ENVIRONMENT AND POLLUTION CONTROL 2020

# Fluxes and mechanisms of phosphorus release from sediments in seasonal hypoxic reservoirs: a simulation-based experimental study

Xiaohong Yang[1,2] · Ruixue Zhang[1] · Jingfu Wang[2,3] · Kangkang He[1,2] · Jingan Chen[2,3]

Received: 15 January 2021 / Accepted: 7 April 2021


## Abstract

**Purpose** Internal phosphorus (P) input has been proven to be an important cause of eutrophication. The purpose of this study is to explore the process and mechanism of P release from sediments in seasonal hypoxic reservoirs.

**Material and methods** Six sediment cores were collected from Hongfeng Reservoir, one of the largest reservoirs in southwestern China. Incubation experiments were conducted using the sediment cores under aerobic and anaerobic conditions. The diffusion gradients in thin films (DGT) technique was employed to determine the concentration profiles and release characteristics of labile-P and labile-Fe at the sediment–water interface. The microbial community structure in surface sediments was determined by 16S rRNA sequencing.

**Results and discussion** Compared with the aerobic condition, the P release flux was ~3.75 times under anaerobic condition, which mainly came from BD-P and NaOH-P. In addition, DGT-P and DGT-Fe were significantly positively correlated ($R^2 > 0.66$, $p < 0.001$). From 16S rRNA sequencing, SRB and PSB were shown to promote P release through sulfate reduction and P dissolution in sediments. Moreover, the control measures of internal P release are discussed due to the potential risk of it in deep-water reservoirs.

**Conclusion** Dissolved oxygen is the key control factor of P release; thus, anaerobic conditions promoted the release of P from sediments. Fe-P reduction and dissolution are the main processes. SRB and PSB played an important role in the P cycle of sediments. It is necessary to increase oxygen in seasonal hypoxic reservoirs to reduce the risk of internal P release.

**Keywords** Internal phosphorus · Seasonal hypoxic reservoir · Sediments · Dissolved oxygen · Diffusive gradients in thin films technique (DGT) · 16S rRNA

## 1 Introduction

Reservoirs are one of the most important storage and utilization forms of freshwater resources in the world. Artificial reservoirs built along the river usually have large water depth (average water depth > 15 m) (Lehner et al. 2011; Maavara et al. 2017). There are more than 45,000 large reservoirs worldwide—defined as reservoirs with dams of more than 15 m (Nilsson et al. 2005). By 2013, 98,002 reservoirs had been built in China with a total capacity of $9.32 \times 10^{10}$ $m^3$ (MWR 2013). Relevant research show that the contribution of reservoirs to the total surface area in China (0.29%) is much larger than the global average (0.17%), and the total capacity of reservoirs (794 $km^3$) is triple that of lakes (268 $km^3$) (Yang and Lu 2014). Therefore, it is very crucial to understand the environmental problems in reservoirs for the regulation and management of water resources.

Eutrophication is one of the most prominent environmental problems in water resources and China's reservoirs are facing increasing eutrophication. Phosphorus (P) is a factor that limits eutrophication in water bodies (Carpenter 2005;

Responsible editor: Haihan Zhang

✉ Jingfu Wang
wangjingfu@vip.skleg.cn

[1] College of Resources and Environmental Engineering, Guizhou University, Guiyang 550025, People's Republic of China

[2] State Key Laboratory of Environmental Geochemistry, Institute of Geochemistry, Chinese Academy of Sciences, Guiyang 550081, People's Republic of China

[3] University of Chinese Academy of Sciences, Beijing 100049, People's Republic of China

Published online: 15 April 2021

Schindler et al. 2016). Therefore, effectively controlling P input into water bodies is essential to addressing the eutrophication problem. The sources of P in water bodies are categorized as external sources (e.g., industrial wastewater, domestic sewage, agricultural non-point sources) and internal sources (sediments release) (Markovic et al. 2019; Ruttenberg 2019; Yang et al. 2020). Under conditions such as hypoxia and wind wave disturbances, P is continuously releasing from sediments to the overlying water, which can become an important "source" of P in water bodies (Ahlgren et al. 2011; Kwak et al. 2018). When the external input is effectively controlled, the continuous input of internal P can maintain the high concentration of P in water (Paytan et al. 2017; Markovic et al. 2019). Therefore, understanding the flux, mechanism, and key control factors impacting how P release from sediments into water bodies. Also, it is of practical significance for internal pollution treatment and eutrophication management in reservoirs.

The coupling between iron (Fe) and P cycles was first proposed by Einsele (1936). It was proposed that P release from sediments is related to the redox of Fe. Many studies have shown that the reduction and dissolution of Fe-P is an important mechanism for the migration and transformation of P in sediments (Smith et al. 2011; Ding et al. 2015; Gao et al. 2016). However, the previous studies on the release process and mechanism of P mainly focused on natural lakes, but few on artificial deep-water reservoirs. Due to its physical structure characteristics, vertical thermodynamic stratification often occurs in deep-water reservoirs. A thermocline forms at a depth of several meters (Henry 1999). In deep-water reservoirs, organic matter, such as algae, that is produced in the surface water continuously sinks to the lower water. When accompanied by organic matter degradation and other oxygen-consuming processes, the DO levels gradually decrease in the bottom water, resulting in an hypoxic state in the deep water (Dutton et al. 2018). In addition, the thermocline hinders the mass transfer process of oxygen to the lower water body, further aggravating the hypoxic condition of the lower static water layer. This positive feedback effect may accelerate the recycling of P and maintain the eutrophication in deep-water reservoir. Therefore, hypoxia has become a common problem in deep-water reservoirs. In these deep-water reservoirs with seasonal hypoxic, the source, migration process, and mechanism of P release needs to be studied.

In this study, parallel sediment column cores were collected from Hongfeng Reservoir, a deep-water and seasonal hypoxic reservoir with periodic eutrophication issues in southwestern China. Using simulated aerobic and anaerobic conditions, experiments assessed the P release process at the sediment–water interface (SWI). The diffusive gradients in thin films technique (DGT) and traditional chemical sequential extraction were used to measure the chemical composition, profile distribution, and temporal variations in P and Fe in sediments and pore water. At the same time, 16S rRNA amplicon sequencing technology was used to analyze the microbial community composition of surface sediments. The objectives of this study were to (1) identify the process and mechanism involved in the release of P from sediments in a seasonal hypoxic reservoir, (2) explore the role and influence of microorganisms in sediments P cycling, and (3) explore the engineering measures that could control internal P release from sediment.

## 2 Materials and methods

### 2.1 Study area

Hongfeng Reservoir (26° 30′ N, 106° 23′ E) is one of the largest artificial reservoirs in southwestern China. It was built in the 1960s, and has a water surface area of 57.2 $km^2$, a water storage capacity of $6.01 \times 10^8$ $m^3$, and an average water depth of 10.5 m (the deepest depth is 45 m). The drinking water source is provided by Hongfeng Reservoir for Guiyang city, with a population of more than 4.8 million. Since the construction, Hongfeng Reservoir has experienced the transformation from eutrophication to mesotrophic. However, in recent years, abnormal partial water quality occurs usually (Guo et al. 2020). Field monitoring showed that the reservoir's water body experiences seasonal stratification, with DO concentration in the bottom water at levels below 1 mg $L^{-1}$ from late spring to early autumn. In other seasons, the bottom water is in an aerobic state (the average DO concentration is approximately 6 mg $L^{-1}$) (Wang et al. 2016). Due to seasonal hypoxia, internal P input has become an important source of increased P concentrations in the Hongfeng Reservoir (Wang et al. 2016; Chen et al. 2019b).

### 2.2 Sample collection and simulation experiment

In September 2019, six sediment column cores were collected from the Dam of Hongfeng Reservoir (DM, 23 m of water depth, Fig. S1) using a gravity sampler (the inner diameter and height of the column core were 11 cm and 50 cm, respectively). The collected column cores were wrapped in aluminum foil to protect them from the light and were brought back to the laboratory. After the cores stabilized, the overlying lake water was siphoned off, and Milli-Q water was slowly added. The ratio of the sediment column core thickness to the overlying water thickness was approximately 2:3 for all the column cores. The conventional physical and chemical parameters of the water profile were detected in situ using a multiparameter water quality monitor (YSI6600V2, YSI Inc., USA) at 1-m intervals.

The sampled parallel column cores were analyzed using laboratory simulation experiments. They were divided into two groups, the aerobic group and anaerobic group, and each

group had three individual column cores. The overlying water was controlled in anaerobic (DO <1 mg $L^{-1}$) and aerobic (DO >6 mg $L^{-1}$) states by continuously injecting pure nitrogen or air. During the experiment, the incubation temperature was controlled at 22 °C ± 1 °C to simulate the temperature of the lake bottom water (Fig. S2). The simulation experiment lasted for 16 days, with the simulation device was maintained in dark condition. During the 16-day experimental period, 200-mL water samples were collected from the overlying water on days 1, 2, 5, 7, 13, and 16. Due to the large sampling volume, a replacement volume of Milli-Q water was added after each sampling event. These volume cores were modified in subsequent calculations. On days 1, 5, 10, and 15, the ZrO-chelex DGT device (Easysensor Ltd., Nanjing, China) filled with nitrogen and oxygen was inserted into the sediment core vertically and slowly, and kept 3 cm in the overlying water for 24 h. At last, the sediment column cores were sampled at 1-cm intervals after the overlying water was extracted. The sediment samples were freeze-dried (FDU-2100, Shanghai Bilon Instrument Co., Ltd.) and ground to particle sizes of below 200 meshes for chemical analysis.

### 2.3 Analysis of hydrochemistry and sediment component

After the ZrO-Chelex DGT was removed, the surface of the ZrO-Chelex gel was rinsed with Milli-Q water. The gel layer was then removed, and cut into small pieces at 2-mm intervals with a ceramic knife (Easysensor Ltd., Nanjing, China). The thin film slices were then transferred to a 1.5-mL centrifuge tube, and were extracted using 1.0 M $HNO_3$ and 1.0 M NaOH for a 16-h elution period to extract the liable-Fe (DGT-Fe) and liable-P (DGT-P) (Ding et al. 2015). The Fe and P concentrations in the eluate were measured using the phenanthroline colorimetric method (Tamura et al. 1974) and the molybdenum blue method (Murphy and Riley 1962), respectively, using an Epoch microplate spectrophotometer (BioTek, USA). The concentration of soluble reactive phosphorus (SRP) in the overlying water sample was measured using the molybdenum blue method (Murphy and Riley 1962).

After the simulation experiment, the surface sediment in the upper 5 cm was sampled at 1-cm intervals. The Hupfer method was used to extract and measure the relative content of P forms of in the sediments (Hupfer et al. 1995). The TP content in sediment was measured using the $HClO_4$-$H_2SO_4$ digestion method (Frankowski et al. 2002). Mixed acid ($HNO_3$-HCl-HF) was used to digest the sediments; then, an inductively coupled plasma optical emission spectrometer (ICP-OES; Vista MPX, Varian, USA) was used to analyze iron (Fe), aluminum (Al), calcium (Ca), and manganese (Mn) contents in the sediments. All samples were treated overnight with 1 M HCl to remove carbonate (Midwood and Boutton 1998). The total organic carbon (TOC) and total nitrogen (TN) were measured using an element analyzer (Elementar , Vario MACRO cube, DEU).

### 2.4 DNA extraction and microbial community analysis

Fresh surface sediment samples, at 1 cm in size each, were collected and placed in sterile centrifuge tubes. The refrigerated samples were tested by Sangon Biotech Co., Ltd. (Shanghai, http://www.life-biotech.com/). After DNA extraction, PCR amplification, and 16S sequencing, the microbial community structure was obtained. The DNA was extracted using an OMEGA kit EZNA Mag-Bind Soil DNA Kit extraction kit. Then, the DNA integrity and concentrations were tested using agarose gel. The qubit 2.0 DNA detection kit was used to accurately quantify the genomic DNA, and then it was sequenced after mixing with the same amount of 1:1. When the same amount of DNA was mixed, the DNA volume of each sample was 10 ng, and the final sequencing concentration on the computer was 20 pmol. Then, samples were used for PCR amplification; the amplified region was the V3–V4 region of 16S rRNA. After PCR, the PCR products were detected using electrophoresis using agarose gel. Clean reads were generated after sequencing using the Misdq platform.

To study the species composition of each sample, the sequences were clustered into operational taxonomic units (OTUs) at a similarity level of 97%. Clean reads with a uniform sequencing depth were used to annotate classification information of microbial species based on OTUs using QIIME platform. A RDP Classifier algorithm was used to annotate species classification information from the phylum level to the genus level. Based on the species abundance in each sample, the software Mothur was used to calculate the population richness indexes (Chao index and ACE index) and the community diversity indexes (Shannon index and Simpson index).

### 2.5 Data analysis

To quantify the P release from sediments, the internal P input flux in the sediment column cores of the aerobic and anaerobic groups were calculated using a method based on changes in the P concentration in the overlying water over time. This was done by calculating the P release rate from sediments (mg $m^{-2}$ $day^{-1}$, Eq (1)) (Fisher and Reddy 2001) using the changes in the P concentration in the overlying water of the sediment column cores over time, as follows:

$$F = \frac{\left[V(C_n - C_0) + \sum_{j=1}^{n} V_{j-1}\left(C_{j-1} - C_a\right)\right.}{A \times t} \quad (1)$$

In which, $V$ denotes the volume of the overlaying water (L) of the bottom sludge column; $V_{j-1}$ denotes the volume (L) of

the water sample taken at $j$-1 time; $C_0$, $C_n$, and $C_{j\text{-}1}$ denote the P concentration (mg $L^{-1}$) of the water sample taken at 1, $n$ and $j$-1 time, respectively; $C_a$ denotes the P concentration (mg $L^{-1}$) in the supplement water; $A$ denotes the surface area ($m^2$) of the sediments; and $t$ denotes the temporal cycle (d).

The concentration of liable-P and liable-Fe (II) in the sediments obtained using DGT was calculated (Xu et al. 2013) using Eq (2) as follows:

$$C_{DGT} = \frac{M_{\Delta g}}{D_{\Delta t}} \quad (2)$$

where $M$ denotes the cumulative amount of P in the fixed film (ng); Δg denotes the thickness of the diffusion layer (cm); $D$ denotes the diffusion coefficient of P in the diffusion layer ($cm^2$ $s^{-1}$); $A$ denotes the area of each strip film ($cm^2$, resolution width is 1 cm × 2 cm); and $t$ denotes the placement time of the DGT device.

### 2.6 Statistical analysis

SPSS 23.0 (IBM Corp. USA) was utilized to complete the statistical analysis. The analysis included determining the Pearson correlation coefficient and analyzing the correlation between DGT-P and DGT-Fe. Origin 2017 (Origin Lab Inc., USA) and R (Version 3.1) were used for the plotting process. Userach software (Uparse Version 5.2.236) was used for the cluster analysis of the clean reads. Mothur software (Version 1.30.1) was used to calculate the diversity index.

## 3 Results

### 3.1 The effects of DO on the concentration of in overlying water

Figure 1 shows the change of SRP in the overlying water of sediment column cores with time under different treatment conditions. For the anaerobic group, the SRP concentration in the overlying water increased continuously from 0.08 ± 0.01 mg $L^{-1}$ on 1 day to 0.15 ± 0.05 mg $L^{-1}$ on 16 days. The SRP concentration of the aerobic group increased slightly to 0.03 ± 0.02 mg $L^{-1}$, but it was significantly lower compared to the anaerobic group. Based on the temporal variation in the SRP concentration in the overlying water the column cores, the internal P release flux (Eq (1)) in the sediment column cores was calculated under the two different conditions. The release flux of sediments P in the column cores of the aerobic group was significantly smaller compared to the anaerobic group, which was 0.69 ± 0.43 mg $m^{-2}$ $day^{-1}$ and 2.59 ± 1.34 mg $m^{-2}$ $d^{-1}$, respectively. These results indicate that anaerobic conditions facilitate P release from sediments.

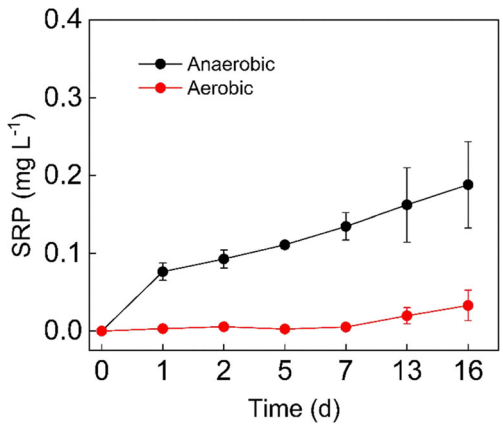


**Fig. 1** Changes in the SRP concentration in overlying water under different DO conditions

### 3.2 Changes in P content of different forms in sediments

To study the potential of P release from sediments, the changes in the content of P forms in the 0–5 cm surface sediments under different treatment conditions were determined (Fig. 2, Table 1). Under different conditions, the content of P forms was ranked as follows: NaOH-P > residual-P > HCl-P > BD-P > $NH_4Cl$-P. The NaOH-P was dominant, at content of 569.77–707.62 mg $kg^{-1}$ in the aerobic samples and 488.99–543.85 mg $kg^{-1}$ in the anaerobic samples, accounting for 42.23 ± 2.2% and 38.32 ± 4.3% of TP, respectively. Then, it was residual-P at content of 218.58–245.73 mg $kg^{-1}$ (aerobic) and 214.86–233.37 mg $kg^{-1}$ (anaerobic), and HCl-P at content of 172.31–224.64 mg $kg^{-1}$ (aerobic) and 194.45–259.36 mg $kg^{-1}$ (anaerobic). The $NH_4Cl$-P content was lowest in all cores, with an average level of 5.35 mg $kg^{-1}$ (aerobic) and 10.54 mg $kg^{-1}$ (anaerobic). This accounted for only approximately 1% of the TP.

After the simulation experiment, the TP content of the aerobic group was higher compared with the anaerobic group (1478.14 > 1352.86 mg $kg^{-1}$, ave). The content of BD-P and NaOH-P in the anaerobic sample group was significantly lower compared with those of the aerobic sample group. The content of $NH_4Cl$-P and HCl-P exhibited an opposite trend. In addition, there were no significant changes in the P forms in the different layers.

### 3.3 Temporal variation of DGT-P and DGT-Fe concentration profiles

The concentration profiles of DGT-P/Fe (according to Eq (2)) with time and depth under the two conditions (aerobic and anaerobic) is presented in Fig. 3. DGT-P (Fe) increased as the depth increased. At the same time, the DGT-Fe value was higher that the DGT-P. Under the aerobic condition (DO >6 mg $L^{-1}$), the changes of DGT-Fe and DGT-P became increasingly stable as the cultivation time increased; a similar

**Table 1** Basic parameters of surface sediment samples under aerobic and anaerobic conditions

| Condition | Depth (cm) | TOC (%) | TN (%) | Fe (g $kg^{-1}$) | Al (g $kg^{-1}$) | Ca (g $kg^{-1}$) | Mn (g $kg^{-1}$) | $NH_4Cl$-P (mg $kg^{-1}$) | BD-P (mg $kg^{-1}$) | NaOH-P (mg $kg^{-1}$) | HCl-P (mg $kg^{-1}$) | Residual-P (mg $kg^{-1}$) | Total-P (mg $kg^{-1}$) |
|---|---|---|---|---|---|---|---|---|---|---|---|---|---|
| Aerobic | −1 | 7.93 | 0.92 | 40.26 | 56.77 | 34.22 | 0.77 | 4.68 | 144.12 | 569.77 | 172.32 | 226.28 | 1310.61 |
| | −2 | 7.75 | 0.89 | 37.90 | 53.84 | 32.96 | 0.75 | 5.17 | 157.04 | 678.67 | 174.37 | 229.26 | 1541.88 |
| | −3 | 7.01 | 0.80 | 29.97 | 42.79 | 26.18 | 0.60 | 7.85 | 173.37 | 707.62 | 207.34 | 218.58 | 1612.64 |
| | −4 | 6.93 | 0.77 | 34.08 | 48.35 | 28.68 | 0.70 | 4.54 | 197.09 | 577.30 | 205.60 | 227.23 | 1478.89 |
| | −5 | 6.62 | 0.77 | 57.15 | 77.65 | 43.52 | 1.13 | 4.52 | 182.63 | 589.21 | 224.64 | 245.73 | 1446.66 |
| | Ave | 7.25 | 0.83 | 39.87 | 55.88 | 33.11 | 0.79 | 5.35 | 170.85 | 624.51 | 196.85 | 229.42 | 1478.14 |
| Anaerobic | −1 | 8.05 | 0.86 | 23.17 | 34.12 | 22.21 | 0.49 | 12.27 | 133.27 | 526.34 | 194.45 | 221.81 | 1187.21 |
| | −2 | 7.43 | 0.85 | 30.00 | 40.69 | 27.75 | 0.58 | 7.94 | 140.59 | 499.99 | 195.53 | 214.86 | 1411.07 |
| | −3 | 7.51 | 0.83 | 43.78 | 60.54 | 33.87 | 0.86 | 8.74 | 144.46 | 488.99 | 211.77 | 229.07 | 1487.90 |
| | −4 | 7.29 | 0.80 | 36.35 | 50.42 | 28.50 | 0.74 | 9.42 | 188.62 | 510.80 | 219.10 | 233.37 | 1389.78 |
| | −5 | 7.13 | 0.72 | 38.65 | 52.68 | 29.09 | 0.79 | 14.31 | 156.76 | 543.85 | 259.36 | 226.69 | 1288.33 |
| | Ave | 7.48 | 0.81 | 34.39 | 47.69 | 28.28 | 0.69 | 10.54 | 152.74 | 513.99 | 216.04 | 225.16 | 1352.86 |

outcome was seen under anaerobic condition (DO <1 mg $L^{-1}$). The correlation between DGT-Fe and DGT-P was stronger in the anaerobic condition compared to aerobic (0.83 > 0.74, ave). Figure 3 shows that under anaerobic condition, as the depth and time changed, the DGT-Fe concentration increased significantly, and it was much higher than under the aerobic condition. The change of DGT-Fe was smaller under the aerobic condition. Under the two conditions, the DGT-P concentration changed little with time. The DGT-P (Fe) concentration changed on the vertical profile as follows: 20–10 mm was the stable stage, and 10–200 mm was the increasing stage. At the same time, the SWI of the anaerobic group had a higher concentration of DGT-P compared to the aerobic group (0.142 > 0.009 mg $L^{-1}$, 15 days). At the same time, the linearity of DGT-P and DGT-Fe showed a significant positive correlation between the DGT-P and DGT-Fe concentrations ($R^2 > 0.66$, $p < 0.001$, Fig. 4).

### 3.4 Analysis of microbial community structure

A bacterial community analysis was performed on the six sediment column cores. After quality screening and cutting, they were assigned to 30,823 OTUs. At a 97% similarity level, a sample OTU, goods coverage, richness, and diversity of the bacterial community are shown in Table 2. The average sequencing coverage rate exceeded 91%, indicating that sequencing covered all microbial communities. There were 36 phylum, 83 classes, 128 orders, 226 families, and 350 genera

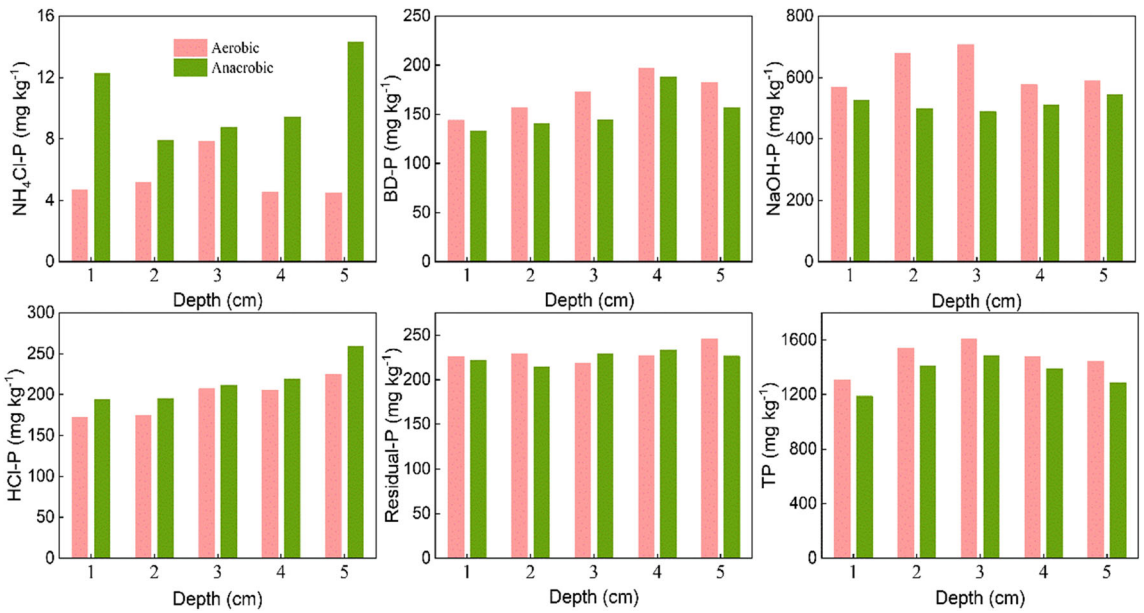


**Fig. 2** Changes in sediment P levels under different treatment conditions

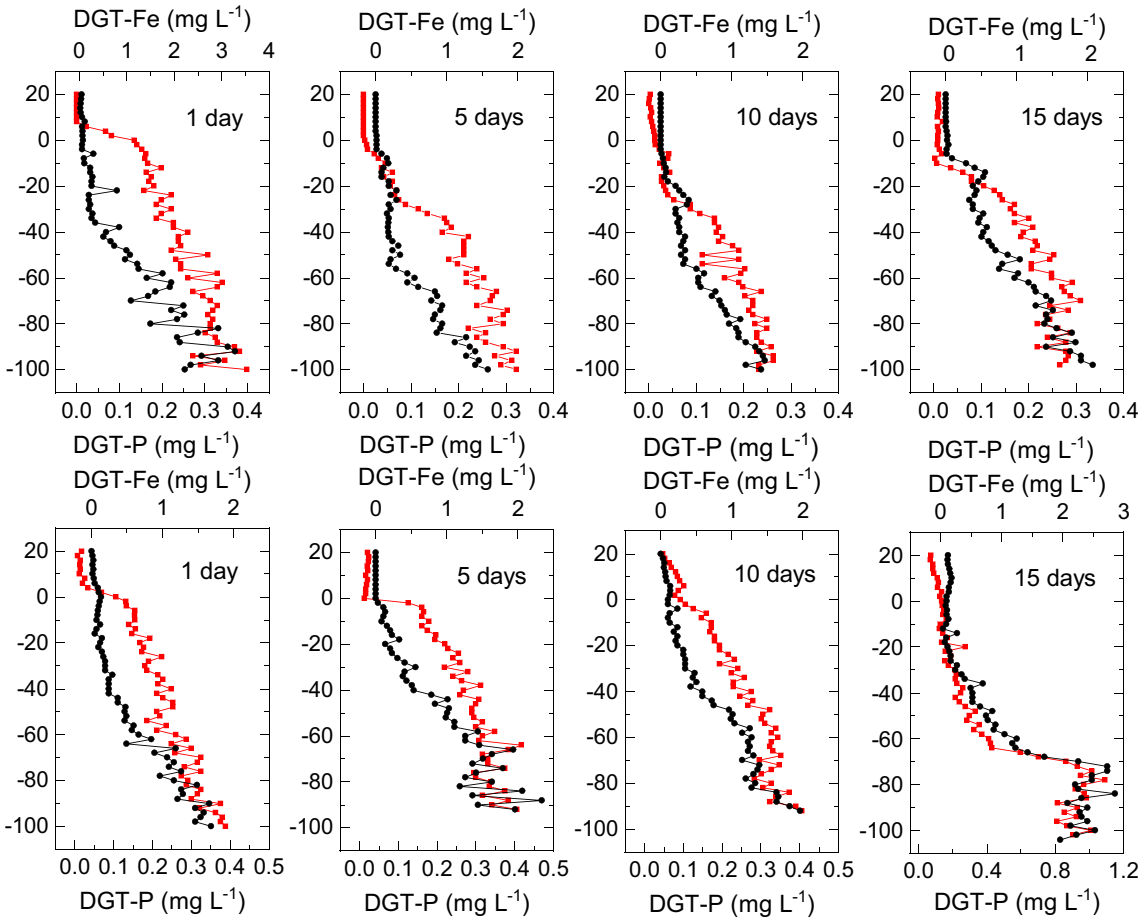


**Fig. 3** Profile changes for DGT-P and Fe concentrations with time and depth under different treatment conditions

detected, demonstrating the diversity of microbial communities. The community richness of the anaerobic group exceeded that of the aerobic group (Chao, ACE). The Shannon and Simpson indexes indicated there was not much difference in the community diversity between the aerobic and anaerobic groups.

The bacterial community composition was detected of different samples at the phylum level (Fig. 5). A total of 36 phyla were detected. Among all samples, *Proteobacteria* was the most abundant phylum, accounting for 33% (ave). The remaining phylum at abundances over 1% were as follows: *Planctomycetes* (12.48%), *Chloroflexi* (11.3%),

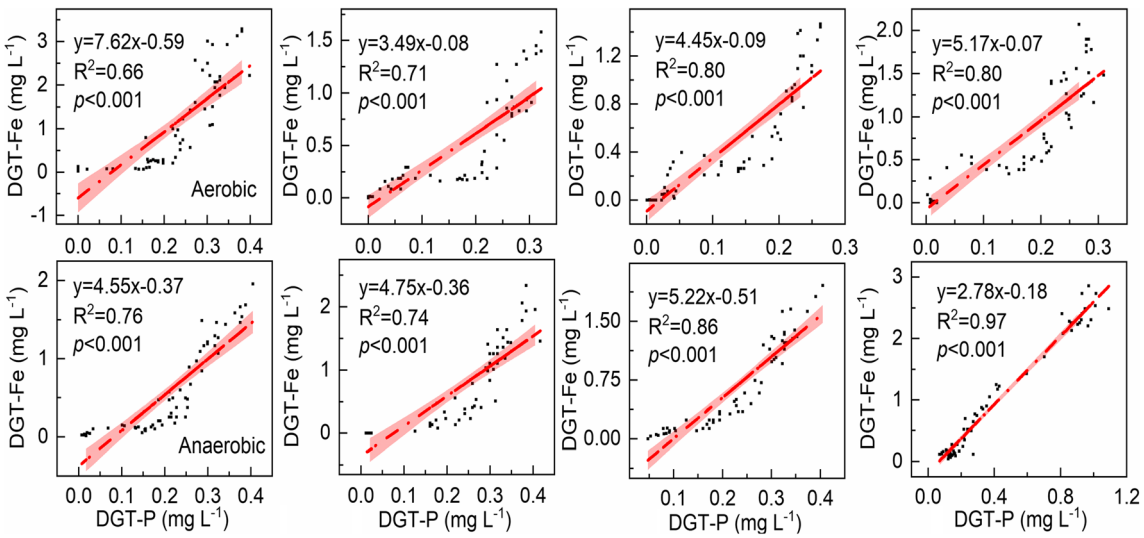


**Fig. 4** Correlation analysis between DGT-P and DGT-Fe

**Table 2** The bacterial community diversity index of sediment samples at 97% similarity level under different treatment conditions (SD-A, B, C are the aerobic groups, SD-D, E, F are the anaerobic groups)

| Sample | OTU | Shannon | ACE | Chao1 | Coverage | Simpson |
|---|---|---|---|---|---|---|
| SD-A | 4781 | 7.05 | 11,845 | 8594 | 0.91 | 0.0033 |
| SD-B | 5213 | 7.02 | 12,461 | 9253 | 0.92 | 0.0043 |
| SD-C | 5321 | 7.14 | 12,042 | 9103 | 0.92 | 0.0041 |
| SD-D | 5117 | 7.16 | 12,900 | 9353 | 0.91 | 0.0036 |
| SD-E | 5088 | 7.12 | 12,492 | 9119 | 0.91 | 0.0031 |
| SD-F | 5302 | 7.19 | 12,119 | 9031 | 0.92 | 0.0030 |

*Verrucomicrobia* (9.46%), *Acidobacteria* (7.57%), *Bacteroidetes* (6.27%), *Actinobacteria* (5.58%), *Firmicutes* (4.31%), *Chlamydiae* (2.32%), *Parcubacteria* (1.31%), and *Aminicenantes* (1.11%). There was no obvious difference between the aerobic group and the anaerobic group with respect to microbial species; however, there were differences in the relative proportions of specific bacterial species (Fig. 5). The bacteria present were closely related to the nutrient cycle of sediments.

The bacterial communities associated with P cycling in sediments were analyzed (Table 3). A total of 350 genera were detected in the sediments. A total of 21 genera were found by searching for desulfurization bacteria within the monitored genera (Table 3). The relative abundance of bacteria did not significantly difference between the anaerobic and aerobic groups. At the same time, it was found that there were 8 genera of phosphate-solubilizing bacteria (PSB): *Geobacter*, *Pseudomonas*, *Acinetobacter*, *Achromobacter*, *Rhizobium*, *Flavobacterium*, *Azospirillum*, *Bacillus*.

## 4 Discussion

### 4.1 The effect of DO on phosphorus release from sediments

In this study, different concentrations of DO have different effects on P release from sediments. The P concentrations in the overlying water and the P release flux from the core under anaerobic condition were significantly higher than those under aerobic condition (Fig. 1), indicating that anaerobic promoted the release of P from sediment to the overlying water. This is mainly because at low DO levels, the Fe (III) is reduced to Fe (II) in the surface sediments at the SWI, accompanied by the reduction and dissolution of Fe-P in the sediments. Thus, free SRP diffuses to the SWI, increasing the overlying water SRP concentration (Fig. 1). Under aerobic condition, Fe(II) is easily oxidized to Fe(III) to form Fe(OOH) compounds. This process provides a large number of free adsorption sites for P ions ($PO_4^{3-}$) in water and sediment, thus forming Fe(OOH)-P complexes, which hinder the release of internal P (Och et al. 2012; Nóbrega et al. 2014; Markovic et al. 2019). The significant correlation between DGT-Fe and DGT-P in sediments ($R^2 > 0.66$, $p < 0.001$) (Figs 3, 4) indicated that liable-P and liable-Fe in the sediments were simultaneously released from sediments. This indicates that the release of P from Hongfeng Reservoir sediments is mainly controlled by the reduction and dissolution of Fe-P, which is consistent with the results of in situ experiments (Chen et al. 2019b). The release of P from sediments is mainly characterized by the change of P forms (Jin et al. 2006; Tang et al. 2013). $NH_4Cl$-P, BD-P, and NaOH-P are considered to be unstable forms of P and are

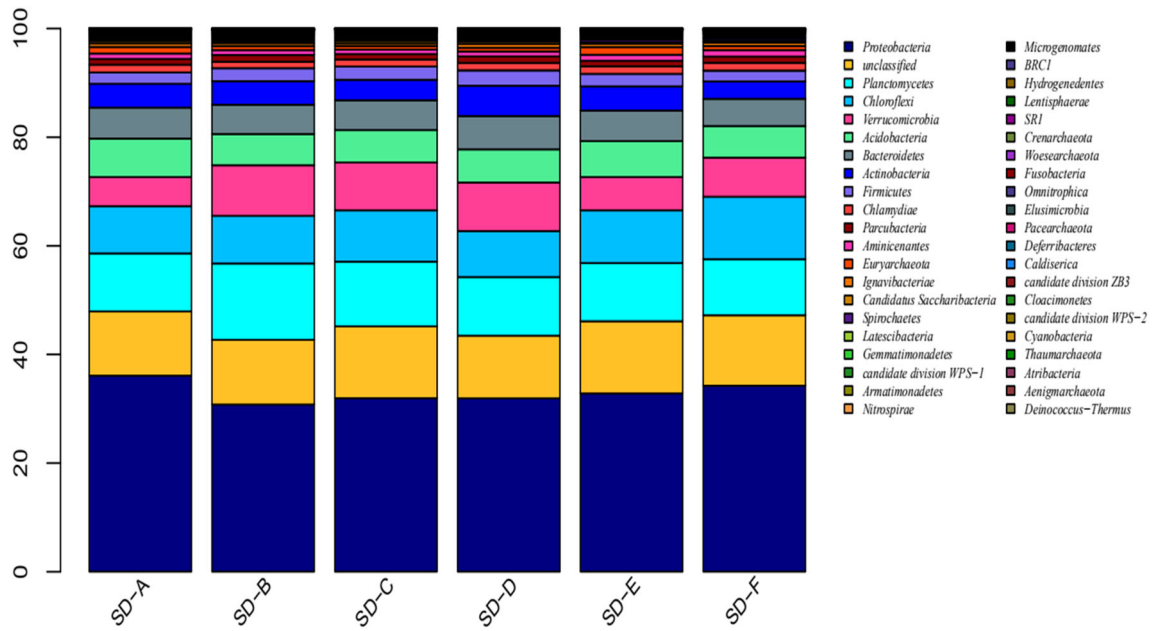


**Fig. 5** Column graphs of the relative abundance of species at the phylum level (SD-A, B, C represent the aerobic groups, SD-D, E, F represent the anaerobic groups)

**Table 3** Bacterial communities associated with the P cycle at the genus level

| Cycling processes | Genus | Aerobic (%) | Anaerobic (%) |
|---|---|---|---|
| Sulfur | Desulfatiglans | 0.503 | 0.632 |
| | Desulfatirhabdium | 0.542 | 0.468 |
| | Thiobacillus | 0.558 | 0.460 |
| | Desulfomonile | 0.190 | 0.172 |
| | Desulfonatronobacter | 0.114 | 0.119 |
| | Desulfocapsa | 0.109 | 0.108 |
| | Desulfobacca | 0.101 | 0.103 |
| | Desulforhabdus | 0.050 | 0.072 |
| | Desulfovirga | 0.053 | 0.073 |
| | Desulfobulbus | 0.052 | 0.064 |
| | Sulfurimonas | 0.029 | 0.046 |
| | Desulfosarcina | 0.037 | 0.030 |
| | Desulfatitalea | 0.022 | 0.028 |
| | Desulfuromonas | 0.017 | 0.021 |
| | Thermodesulfovibrio | 0.009 | 0.010 |
| | Desulfovibrio | 0.008 | 0.013 |
| | Desulfonema | 0.009 | 0.008 |
| | Desulfobacula | 0.007 | 0.007 |
| | Desulfoprunum | 0.008 | 0.006 |
| | Desulfofaba | 0.004 | 0.012 |
| | Desulfitobacterium | 0.002 | 0.007 |
| Phosphorus | Geobacter | 0.083 | 0.072 |
| | Pseudomonas | 0.083 | 0.049 |
| | Acinetobacter | 0.052 | 0.050 |
| | Achromobacter | 0.003 | 0.011 |
| | Rhizobium | 0.004 | 0.008 |
| | Azospirillum | 0.003 | 0.003 |
| | Flavobacterium | 0.107 | 0.124 |
| | Bacillus | 0.051 | 0.052 |
| Total | | 2.361 | 2.879 |

easily released from sediments (Rydin 2000; Yang et al. 2020). The content of TP in sediment under anaerobic condition was lower than that under aerobic condition, which difference was mainly due to the BD-P and NaOH-P in the sediments (Table 1, Fig. 2). In addition, the high content of liable-P in SWI under anaerobic condition is an evidence of P release from sediments (Fig. 3).

The release of P from sediments is a complex process involving many microscopic physical, chemical, and biological processes at the SWI, such as DO, temperature, pH, and microbial (Jin et al. 2006; Sinkko et al. 2013; Gibbons and Bridgeman 2020; Gu et al. 2020). In lake ecosystems, many studies have shown that DO and Fe redox reactions and are important in P exchange between water and sediment (Wang et al. 2008; Wu et al. 2014; Kang et al. 2018; Tammeorg et al. 2020).

Sulfate reduction process can promote the release of P from the sediment, which comes from Fe-P (Chen et al. 2016; Wu et al. 2018). Ca-P is easier to release in acid condition (pH < 7), while when pH > 7, the release of Fe-P usually occurs (Jin et al. 2006). Fe but not Mn redox reactions should control mobilization of P in Meiliang Bay sediments of Taihu Lake, the third largest shallow freshwater lake in China (Chen et al. 2019a). However, the redox of Mn is more important for the release of P, rather than Fe, in Aha Reservoir, a seasonal hypoxic reservoir in southwest China (Sun et al. 2017) and Chen et al. (unpublished data). In short, the dissolution of Fe-P does not dominate the internal P loading in all seasonal hypoxic reservoirs, but which is still the most widely recognized.

### 4.2 The influence of microorganisms on the release of P from sediments

Dissolved oxygen is very important for P release from sediments. However, microorganisms are also key drivers to shape the P cycle in the earth's environment. Studies have shown that microorganisms directly or indirectly affect the release of P from sediments (Wu et al. 2008; Gu et al. 2020). Pomeroy et al. (1965) also noted that the release of P from sediments under the presence of microorganisms is 50% to 100% higher compared with the aseptic condition. The level of P released by biological metabolism is more than five times higher than the physical and chemical processes (Qian et al. 2011). It shows that the role of microorganisms in the P cycle of sediments cannot be ignored. The results of 16S rRNA sequencing showed that the sediment microbial community was rich and contained many microorganisms related to nutrient load (Fig. 5, Table 3).

Iron-reducing bacteria (IRB) and sulfate-reducing bacteria (SRB) play an important role in sediment P cycling (Ma et al. 2017; Wu et al. 2019). Previous studies have shown that hypoxia promotes the growth of IRB and SRB (Roden and Zachara 1996). IRB such as *Geobacter*, *Ferribacterium limneticum*, *Paludibaculum fermentans*, and *Anaeromyxobacter dehalogenans* speed up Fe(III) reduction process in the sediments under hypoxic conditions (Lovley et al. 1998; Cummings et al. 1999; Voordeckers et al. 2010; Bai et al. 2019). However, in this study, the presence of IRB was not observed. On the contrary, SRB was detected in the sediment microbial community, such as *Desulfovibrio*, *Desulfobacterales*, *Desulfatiglans*, *Desulfuromonadales*, *Desulfobacca*, *Desulfovibrionales*, and *Desulfobulbus* (Table 3). In this study, SRB may promote the reduction of Fe(III). SRB anaerobic respiration dissimilates and reduces sulfate to produce $S^{2-}$ and $H_2S$. This facilitates the production of iron sulfide (FeS), reducing Fe(III), and indirectly inducing the desorption and release of Fe-P in the sediments (Sinkko et al. 2013; Wang et al. 2016). Previous studies on the effect of microorganisms on P release in sediments of Hongfeng

Reservoir also focused on SRB rather than IRB (Wang et al. 2016; Chen et al. 2019b).

PSB have been considered to play vital role in the process of P cycling in freshwater ecosystems (Qian et al. 2010; Liu et al. 2017; Li et al. 2021), which can accelerate the P cycling by degrading organic P and releasing inorganic P (Qu et al. 2013; Maitra et al. 2015; Liu et al. 2017; Li et al. 2019). In this study, eight typical PSB, including *Geobacter*, *Pseudomonas*, *Acinetobacter*, *Achromobacter*, *Rhizobium*, *Flavobacterium*, *Azospirillum*, and *Bacillus*, were observed at the genus level (Table 3). For the lake environment, different kinds of PSB have been isolated and identified, and the ability of P release has been proved (Kim et al. 2005; Wu and Zhou 2005). The common PSB in sediments are summarized in Table 4. The results show that PSB can promote the release of P in sediments during P regeneration cycle (Qu et al. 2013; Maitra et al. 2015; Li et al. 2021). PSB solubilizes P in sediments of the Three Gorges Dam, the biggest water conservancy project in the world, to improve recognization of its role in P cycling in large reservoirs (Liu et al. 2017). Ca-P is considered to be the main form of P solubilizes by PSB (Maitra et al. 2015). HCl-P can also be released from sediments by many strains of inorganic PSB, showing a strong ability of P release (Li et al. 2019). Moreover, inorganic PSB release more P than organic PSB (Qian et al. 2010). There are many opinions about the mechanism of phosphate solubilizing of PSB, the production of organic acids has been focused. This reduces the pH value of the environment, leading to the degradation of insoluble phosphates into available P. Alternatively, organic acids can chelate and dissolve metal ions in Fe-P, Al-P, and Ca-P (Chen et al. 2006; Panda et al. 2016). At the same time, PSB also has the characteristics of P mineralization. The complex mechanism of phosphate-solubilizing leads to less attention, but the impact on P cycle cannot be ignored. In addition, the composition of bacteria in sediments is a complex system. In this study, it was found that there was a strong correlation between bacterial community and different P forms at genus level, such as *Pseudomonas*, *Desulfobacca*, *Acinetobacter*, and *Comamonas*, and so on associated with NaOH-srp, *Desulfobulbus* associated with HCl-P, *Parachlamydia* associated with BD-P and TP, and so on (Fig.S3). Therefore, the specific effects of microorganisms on P cycling in sediments need to be further studied.

### 4.3 Prevention and control measures for managing P pollution from sediments in engineering applications

The release of internal P pollution in sediments should be concerned. In this study, the fluxes from sediments (aerobic: 0.69 ± 0.43 mg $m^{-2}$ $day^{-1}$, anaerobic: 2.59 ± 1.34 mg $m^{-2}$ $day^{-1}$) was remarkably high than those from eutrophication lakes, such as Dongting Lake (−0.027 mg $m^{-2}$ $day^{-1}$–−0.197 mg $m^{-2}$ $day^{-1}$, mean: 0.086 mg $m^{-2}$ $day^{-1}$) and Chaohu Lake (0.37 mg $m^{-2}$ $day^{-1}$–2.17 mg $m^{-2}$ $day^{-1}$) (Gao et al. 2016; Li et al. 2020a), which indicating the seriousness of the internal P pollution in Hongfeng Reservoir. Although many shallow Lakes are facing serious eutrophication problems, the level of internal P pollution in lakes is lower than that in deep-water reservoirs. For example, the TP content in sediments of Chaohu Lake ranges from 343 to 1746 mg $kg^{-1}$, (mean: 898 mg $kg^{-1}$). However, the TP content of deep-water reservoirs in Southwest China is relatively high, such as Hongfeng Reservoir (range: 766–4306 mg $kg^{-1}$, mean: 1815 mg $kg^{-1}$), AHa Reservoir (range: 1050–1960 mg $kg^{-1}$, mean 1415 mg $kg^{-1}$) and Zipingpu Reservoir (range: 682.39–1609.06 mg $kg^{-1}$, mean: 1121.08 mg $kg^{-1}$) (Wang et al. 2015; Chen et al. 2018; Wang et al. 2019; Yang et al. 2020). These

**Table 4** Summary of common phosphate solubilizing bacteria (PSB) in sediments

| Genus | References | Genus | References |
|---|---|---|---|
| *Enterobacter* | (Qian et al. 2010; Su et al. 2019) | *Micromonospora* | (El-Tarabily and Youssef 2010) |
| *Bacillus*<br>*Paenibacillus* | (Paul and Sinha 2013; Li et al. 2019) | *Aminobacter*<br>*Arthrobacter* | (Liu et al. 2017) |
| *Vibrio*<br>*Micrococcus* | (kannapiran and Ramkumar 2011; Paul and Sinha 2013; Su et al. 2019) | *Aeromonas*<br>*Pantoea agglomerans* | (Qian et al. 2010) |
| *Flavobacterium* | | *Rhizobium* | |
| *Corynebacterium* | | *Achromobacter* | |
| *Alcaligenes* | | *Agrobacterium* | |
| *Pseudomonas* | (Venkateswaran and Natarajan 1983) | *Burkholderia* | Lin et al. 2006, Qian et al. 2010) |
| *Azospirillum* | (Wu and Zhou 2005) | *Aeromonas* | (Paul and Sinha 2013) |
| *Acinetobacter haemolyticus* | (Grangeasse et al. 1998) | *Enterobacter aerogenes* | (Lee et al. 2000) |

data indicate that internal P pollution has a huge environmental risk to deep-water reservoirs.

Several methods and measures are currently used to control the input of internal P in lakes. However, P-releasing controlled from sediments remains a challenging task. Sediment dredging (Yu et al. 2017; Oldenborg and Steinman 2019; Li et al. 2020b), in situ immobilization (Yin et al. 2020), aquatic plant restoration (Zhao et al. 2012), in situ adsorption-microbe combination technology (Liu et al. 2020), and aeration are commonly used to control internal pollution. In this study, it indicated that in deep-water reservoirs, the key factor controlling the release of P from sediments is the change in DO levels. Once there is a significantly anoxic environment at the SWI in a deep-water reservoir, there is a positive feedback effect, where "oxygen-deficiency in the lower water → enhanced release of internal sediment pollutants → increased primary productivity in lakes → aggravated oxygen-deficiency in the lower water body" (Ingall and Jahnke 1997; Conley et al. 2009). Therefore, it is effective to control internal P inputs by increasing the DO level at the SWI.

In response to P releases from sediments caused by SWI oxygen deficiencies in deep-water reservoirs, many researchers have conducted technology research and development to address this problem. A common measure is artificial aeration, which can increase the DO levels in the water body. Widely used deep-water aeration technologies include Speece conical technology (Speece 1971), bubble plume diffusion technology (McGinnis et al. 2004), artificial de-layer technology (Serra et al. 2007), and gas lift technology. These technologies focus on increasing the DO levels of the lower layers of the water body. In recent years, some researchers have developed new oxygenation materials (such as oxygen nanobubble modified minerals) by focusing on the effectiveness of oxygenation at the SWI (Shi et al. 2018; Zhang et al. 2018). By directly adding mineral material loaded with oxygen nanobubbles to the sediment surface, the oxygenation can be accurately increased at the SWI to control P releases from sediments. Developing and applying efficient and environment-friendly SWI oxygenation technologies, materials, and equipment could help achieve in situ control of internal P pollution in deep-water reservoirs.

## 5 Conclusions

This study conducted a simulation experiment to investigate flux in the release of P from sediments, and the associated release mechanisms, in a deep-water reservoir. Do is the key control factor of P release in seasonal hypoxic reservoirs, anaerobic conditions promoted the release of P from sediments. The significant positive correlation between DGT-Fe and DGT-P ($R^2 > 0.66$, $p < 0.001$) suggested that the reduction and dissolution of Fe-P dominate the sediment P release. The changes of BD-P and NaOH-P were the main forms of internal P release. 16S rRNA sequencing showed SRB and PSB played an important role in the P cycle of sediments. Eight typical PSB were detected, which were discussed in the process of P cycling in sediments.

Compared with the natural shallow eutrophic lakes such as Dongting Lake and Chaohu Lake, the TP content and release flux in the sediments are relatively high. There is a higher P loading, faster P release rate, and higher pollution potential in deep-water reservoirs of southwest China, which highlights the importance and urgency of controlling internal P pollution in deep-water reservoirs. In addition, there were possible measures discussed for facilitating bottom water oxygenation and internal P pollution control in deep-water reservoirs. The future research and development of efficient and environment-friendly SWI oxygenation technologies will help solve the problem of sediment P pollution.

**Supplementary Information** The online version contains supplementary material available at https://doi.org/10.1007/s11368-021-02946-7.

**Authors' contribution** Xiaohong Yang: conceptualization, methodology, investigation, writing—original draft, writing—review and editing. Ruixue Zhang: investigation, writing—review and editing. Jingfu Wang: conceptualization, methodology, resources, writing—review and editing, funding acquisition. Kangkang He: investigation, formal analysis. Jingan Chen: investigation, writing—review and editing.

**Funding information** This study was sponsored jointly by the Strategic Priority Research Program of CAS (No. XDB40020400), the Chinese NSF Joint Fund Project (No. U1612441), the Chinese NSF project (No. 41773145, 41977296), the Guizhou Science and Technology Project of China (No. [2019]2-9), the Youth Innovation Promotion Association CAS (No. 2019389), and the CAS Interdisciplinary Innovation Team.

## Declarations

**Conflict of interest** The authors declare no competing interests.

## References

Ahlgren J, Reitzel K, Brabandere HD, Goqow A, Rydin E (2011) Release of organic P forms from lake sediments. Water Res 45:565–572

Bai YN, Wang XN, Wu J, Lu YZ, Fu L, Zhang F, Lau TC, Zeng RJ (2019) Humic substances as electron acceptors for anaerobic oxidation of methane driven by ANME-2d. Water Res 164:114935

Carpenter SR (2005) Eutrophication of aquatic ecosystems: bistability and soil phosphorus. Proc Natl Acad Sci U S A 102:10002–10005

Chen YP, Rekha PD, Arun AB, Shen FT, Lai WA, Young CC (2006) Phosphate solubilizing bacteria from subtropical soil and their tricalcium phosphate solubilizing abilities. Appl Soil Ecol 34:33–41

Chen M, Li XH, He YH, Song N, Cai HY, Wang C, Li YT, Chu HY, Krumholz LR, Jiang HL (2016) Increasing sulfate concentrations

result in higher sulfide production and phosphorous mobilization in a shallow eutrophic freshwater lake. Water Res 96:94–104
Chen JA, Wang JF, Guo JY, Yu J, Zeng Y, Yang HQ, Zhang RX (2018) Eco-environment of reservoirs in China: characteristics and research prospects. Prog Phys Geogr 42:185–201
Chen MS, Ding SM, Wu YX, Fan XF, Jin ZF, Tsang DCW, Wang Y, Zhang CS (2019a) Phosphorus mobilization in lake sediments: experimental evidence of strong control by iron and negligible influences of manganese redox reactions. Environ Pollut 246:472–481
Chen Q, Chen JA, Wang JF, Guo JY, Jin ZX, Yu PP, Ma ZZ (2019b) In situ , high-resolution evidence of phosphorus release from sediments controlled by the reductive dissolution of iron-bound phosphorus in a deep reservoir, southwestern China. Sci Total Environ 666:39–45
Conley DJ, BjÖrck S, Bonsdorff E, Carstensen J, Destouni G, Gustafsson BG, Hietanen S, Kortekaas M, Kuosa H, Markus Meier H (2009) Hypoxia-related processes in the Baltic Sea. Environ Sci Technol 43:3412–3420
Cummings DE, Caccavo F, Spring S, Rosenzweig RF (1999) *Ferribacterium limneticum*, gen. nov., sp. nov., an Fe(III)-reducing microorganism isolated from mining-impacted freshwater lake sediments. Arch Microbiol 171:183–188
Ding S, Han C, Wang Y, Yao L, Wang Y, Xu D, Sun Q, Williams PN, Zhang C (2015) In situ, high-resolution imaging of labile phosphorus in sediments of a large eutrophic lake. Water Res 74:100–109
Dutton CL, Subalusky AL, Hamilton SK, Rosi EJ, Post DM (2018) Organic matter loading by hippopotami causes subsidy overload resulting in downstream hypoxia and fish kills. Nat Commun 9: 1951
Einsele W (1936) Über die Beziehungen des Eisenkreislaufs zum Phosphatkreislauf im eutrophen See. Arch Hydrobiol 29:664–686
El-Tarabily AK, Youssef T (2010) Enhancement of morphological, anatomical and physiological characteristics of seedlings of the mangrove *Avicennia marina* inoculated with a native phosphate-solubilizing isolate of *Oceanobacillus picturae* under greenhouse conditions. Plant Soil 332:147–162
Fisher MM, Reddy KR (2001) Phosphorus flux from wetland soils affected by long-term nutrient loading. J Environ Qual 30:261–271
Frankowski L, Bolaek J, Szostek A (2002) Phosphorus in bottom sediments of Pomeranian Bay (Southern Baltic—Poland). Estuar Coast Shelf S 54:1027–1038
Gao Y, Liang T, Tian S, Wang L, Holm PE, Hansen HCB (2016) High-resolution imaging of labile phosphorus and its relationship with iron redox state in lake sediments. Environ Pollut 219:466–474
Gibbons KJ, Bridgeman TB (2020) Effect of temperature on phosphorus flux from anoxic western Lake Erie sediments. Water Res 182: 116022
Grangeasse C, Doublet P, Vincent C, Vaganay E, Riberty M, Duclos B, Cozzone AJ (1998) Functional characterization of the low-molecular-mass phosphotyrosine-protein phosphatase of *Acinetobacter johnsonii*. J Mol Biol 278:339–347
Gu J, Zhang W, Li Y, Niu L, Zhang H (2020) Source identification of phosphorus in the river-lake interconnected system using microbial community fingerprints. Environ Res 186:109498
Guo W, Zhao Y, Li Y, Guo J (2020) Trophic level and its historical evolution in Lake Hongfeng, Southwest China (In Chinese). Chinese J Ecol 39:3371–3378
Henry (1999) Heat budgets, thermal structure and dissolved oxygen in Brazilian reservoirs, Theoretical reservoir ecology and its Applications. International Institute of Ecology, São Paulo, pp 125–151
Hupfer M, Gächter R, Giovanoli R (1995) Transformation of phosphorus species in settling seston and during early sediment diagenesis. Aquat Sci 57:305–324
Ingall ED, Jahnke RA (1997) Influence of water-column anoxia on the elemental fractionation of carbon and phosphorus during sediment diagenesis. Mar Geol 139:219–229
Jin X, Wang S, Pang Y, Wu FC (2006) Phosphorus fractions and the effect of pH on the phosphorus release of the sediments from different trophic areas in Taihu Lake, China. Environ Pollut 139:288–295
Kang M, Peng S, Tian Y, Zhang H (2018) Effects of dissolved oxygen and nutrient loading on phosphorus fluxes at the sediment–water interface in the Hai River Estuary. China Mar Pollut Bull 130: 132–139
Kannapiran E, Ramkumar VS (2011) Isolation of phosphate solubilizing bacteria from the sediments of Thondi coast, Palk Strait, Southeast coast of India. Annals of Biological Research 2:157–163
Kim YH, Bae B, Choung YK (2005) Optimization of biological phosphorus removal from contaminated sediments with phosphate-solubilizing microorganisms. J Biosci Bioeng 99:23–29
Kwak DH, Jeon YT, Hur YD (2018) Phosphorus fractionation and release characteristics of sediment in the Saemangeum Reservoir for seasonal change. Int J Sediment Res 3:250–261
Lee KS, Song SB, Kim KE, Kim YH, Kim SK, Kho BH, Ko DK, Choi YK, Lee YK, Kim CK (2000) Cloning and characterization of the UDP-sugar hydrolase gene (ushA) of *Enterobacter aerogenes* IFO 12010. Biochem Bioph Res Co 269:526–531
Lehner B, Liermann CR, Revenga C, Vörösmarty C, Fekete B, Crouzet P, Döll P, Endejan M, Frenken K, Magome J (2011) High-resolution mapping of the world's reservoirs and dams for sustainable river-flow management. Front Ecol Environ 9:494–502
Li Y, Zhang J, Zhang J, Xu W, Mou Z (2019) Characteristics of inorganic phosphate-solubilizing bacteria from the sediments of a eutrophic lake. Int J Env Res Pub He 16:2141
Li Y, Kuang S, Wang Z, Shen Q, Kang D (2020a) Characteristics and significance of nitrogen, phosphorus and oxygen transportation at the sediment-water interface in east Lake Chaohu (In Chinese). J Lake Sci 32:688–700
Li Y, Wang L, Yan Z, Chao C, Liu C (2020b) Effectiveness of dredging on internal phosphorus loading in a typical aquacultural lake. Sci Total Environ 744:140883
Li H, Song C, Yang L, Qin H, Cao X, Zhou Y (2021) Phosphorus supply pathways and mechanisms in shallow lakes with different regime. Water Res 193:116886
Lin TF, Huang HI, Shen FT, Young CC (2006) The protons of gluconic acid are the major factor responsible for the dissolution of tricalcium phosphate by *Burkholderia cepacia* CC-Al74[J]. Bioresour Technol 97(7):957–960
Liu YQ, Cao X, Li H, Zhou Z, Wang S, Wang Z, Song C, Zhou Y (2017) Distribution of phosphorus-solubilizing bacteria in relation to fractionation and sorption behaviors of phosphorus in sediment of the Three Gorges Reservoir. Environ Sci Pol 24:17679–17687
Liu Z, Zhang Y, Yan P, Luo J, Wu Z (2020) Synergistic control of internal phosphorus loading from eutrophic lake sediment using MMF coupled with submerged macrophytes. Sci Total Environ 731:138697
Lovley D, Fraga J, Blunt-Harris E, Hayes L, Phillips E, Coates J (1998) Humic substances as a mediator for microbially catalyzed metal reduction. Acta Hydrochim Hydrobiol 26:152–157
Ma WW, Zhu MX, Yang GP, Li T (2017) In situ, high-resolution DGT measurements of dissolved sulfide, iron and phosphorus in sediments of the East China Sea: insights into phosphorus mobilization and microbial iron reduction. Mar Pollut Bull 124:400–410
Maavara T, Lauerwald R, Regnier P, Van Cappellen P (2017) Global perturbation of organic carbon cycling by river damming. Nat Commun 8:15347
Maitra N, Manna SK, Samanta S, Sarkar K, Debnath D, Bandopadhyay C, Sahu SK, Sharma AP (2015) Ecological significance and phosphorus release potential of phosphate solubilizing bacteria in freshwater ecosystems. Hydrobiologia 745:69–83
Markovic S, Liang A, Watson SB, Guo J, Mugalingam S, Arhonditsis G, Morley A, Dittrich M (2019) Biogeochemical mechanisms

controlling phosphorus diagenesis and internal loading in a remediated hard water eutrophic embayment. Chem Geol 514: 122–137
Mcginnis DF, Lorke A, Wuest A, Stoeckli A, Little JC (2004) Interaction between a bubble plume and the near field in a stratified lake. Water Resour Res 40:187–203
Midwood AJ, Boutton TW (1998) Soil carbonate decomposition by acid has little effect on δ13C of organic matter. Soil Biol Biochem 30: 1301–1307
Murphy J, Riley JP (1962) A modified single solution method for the determination of phosphate in natural waters. Anal Chim Acta 27: 678–681
Mwr (2013) Bulletin of first national census for water. China WaterPower Press
Nilsson C, Reidy CA, Dynesius M, Revenga C (2005) Fragmentation and flow regulation of the world's large river systems. Science 308:405–408
Nóbrega GN, Otero XL, Macías F, Ferreira TO (2014) Phosphorus geochemistry in a Brazilian semiarid mangrove soil affected by shrimp farm effluents. Environ Monit Assess 186:5749–5762
Och LM, Müller B, Voegelin A, Ulrich A, Göttlicher J, Steiniger R (2012) New insights into the formation and burial of Fe/Mn accumulations in Lake Baikal sediments. Chem Geol:330–331
Oldenborg KA, Steinman AD (2019) Impact of sediment dredging on sediment phosphorus flux in a restored riparian wetland. Sci Total Environ 650:1969–1979
Panda B, Rahman H, Panda J (2016) Phosphate solubilizing bacteria from the acidic soils of Eastern Himalayan region and their antagonistic effect on fungal pathogens. Rhizosphere 2:62–71
Paul D, Sinha NS (2013) Bacteria showing phosphate solubilizing efficiency in river sediment. Electron J Biosciences 1:1–5
Paytan A, Roberts K, Watson S, Peek S, Chuang P-C, Defforey D, Kendall C (2017) Internal loading of phosphate in Lake Erie Central Basin. Sci Total Environ 579:1356–1365
Pomeroy LR, Smith EE, Grant CM (1965) The exchange of phosphate between estuarine water and sediments. Limnol Oceanogr 10:167–172
Qian Y, Shi J, Chen Y, Lou L, Cui X, Cao R, Li P, Tang J (2010) Characterization of phosphate solubilizing bacteria in sediments from a shallow eutrophic lake and a wetland: isolation, molecular identification and phosphorus release ability determination. Molecules 15:8518–8533
Qu JH, Li HF, Chen N, Yuan HL (2013) Biogeochemical function of phosphorus-solubilising bacteria on cycling of phosphorus at the water-sediment interface under laboratorial simulated conditions. Int J Environ Pollut 52:104–116
Roden EE, Zachara JM (1996) Microbial reduction of crystalline iron(III) oxides: influence of oxide surface area and potential for cell growth. Environ Sci Technol 30:1618–1628
Ruttenberg KC (2019) Phosphorus cycle ☆. Encyclopedia of Ocean Sciences (Third Edition) 1:447–460
Rydin E (2000) Potentially mobile phosphorus in Lake Erken sediment. Water Res 34:2037–2042
Schindler DW, Carpenter SR, Chapra SC, Hecky RE, Orihel DM (2016) Reducing phosphorus to curb lake eutrophication is a success. Environ Sci Technol 50:8923–8929
Serra T, Vidal J, Casamitjana X, Soler M, Colomer J (2007) The role of surface vertical mixing in phytoplankton distribution in a stratified reservoir. Limnol Oceanogr 52:620–634
Shi WQ, Pan G, Chen QW, Song LR, Zhu L (2018) Hypoxia remediation and methane emission manipulation using surface oxygen nanobubbles. Environ Sci Technol 25:8712–8717
Sinkko H, Lukkari K, Sihvonen LM, Sivonen K, Leivuori M, Rantanen M, Paulin L, Lyra C (2013) Bacteria contribute to sediment nutrient release and reflect progressed eutrophication-driven hypoxia in an organic-rich continental sea. PLoS One 8:e67061–e67061
Smith L, Watzin MC, Druschel G (2011) Relating sediment phosphorus mobility to seasonal and diel redox fluctuations at the sediment-water interface in a eutrophic freshwater lake. Limnol Oceanogr 56:2251–2264
Speece RE (1971) Hypolimnion aeration. Journal 63:6–9
Su M, Han FY, Wu YL, Yan ZP, Lv ZS, Tian D, Wang SM, Hu SJ, Shen ZT, Li Z (2019) Effects of phosphate-solubilizing bacteria on phosphorous release and sorption on montmorillonite. Appl Clay Sci 181:105227
Sun QQ, Chen JA, Wang JF, Yang HQ (2017) High-resolution distribution characteristics of phosphorous, iron and sulfur across the sediment-water interface of Aha Reservoir (In Chinese). Environ Sci 38:2810–2818
Tammeorg O, Nürnberg G, Horppila J, Haldna M, Niemistö J (2020) Redox-related release of phosphorus from sediments in large and shallow Lake Peipsi: evidence from sediment studies and long-term monitoring data. J Great Lakes Res 46:1595–1603
Tamura H, Goto K, Yotsuyanagi T, Nagayama M (1974) Spectrophotometric determination of iron(II) with 1,10-phenanthroline in the presence of large amounts of iron(III). Talanta 21:314–318
Tang W, Zhang H, Zhang W, Wang C, Shan B (2013) Biological invasions induced phosphorus release from sediments in freshwater ecosystems. Colloid Surface A 436:873–880
Venkateswaran K, Natarajan R (1983) Seasonal distribution of inorganic phosphate solubilising bacteria and phosphatase producing bacteria in Porto Novo waters. Indian J Geo-Mar Sci 12:213–217
Voordeckers JW, Kim BC, Izallalen M, Lovley DR (2010) Role of *Geobacter sulfurreducens* outer surface c-type cytochromes in reduction of soil humic acid and anthraquinone-2,6-disulfonate. Appl Environ Microbiol 76:2371–2375
Wang S, Jin X, Bu Q, Jiao L, Wu F (2008) Effects of dissolved oxygen supply level on phosphorus release from lake sediments. Colloids Surf A Physicochem Eng Asp 316:245–252
Wang JF, Chen JA, Dallimore C, Yang HQ, Dai ZH (2015) Spatial distribution, fractions, and potential release of sediment phosphorus in the Hongfeng Reservoir, southwest China. Lake Reserv Manage 31:214–224
Wang JF, Chen JA, Ding SM, Guo JY, Christopher D (2016) Effects of seasonal hypoxia on the release of phosphorus from sediments in deep-water ecosystem: a case study in Hongfeng Reservoir, Southwest China. Environ Pollut 219:858–865
Wang Y, Li K, Liang R, Han S, Li Y (2019) Distribution and release characteristics of phosphorus in a reservoir in southwest China. Int J Env Res Pub He 16
Wu GF, Zhou XP (2005) Characterization of phosphorus-releasing bacteria in a small eutrophic shallow lake, Eastern China. Water Res 39: 4623–4632
Wu Q, Zhang R, Huang S, Zhang H (2008) Effects of bacteria on nitrogen and phosphorus release from river sediment. J Environ Sci 20:404–412
Wu Y, Wen Y, Zhou J, Wu Y (2014) Phosphorus release from lake sediments: effects of pH, temperature and dissolved oxygen. KSCE J Civ Eng 18:323–329
Wu S, Zhao Y, Chen Y, Dong X, Wang M, Wang G (2018) Sulfur cycling in freshwater sediments: a cryptic driving force of iron deposition and phosphorus mobilization. Sci Total Environ 657:1294–1303
Wu S, Zhao Y, Chen Y, Dong X, Wang M, Wang G (2019) Sulfur cycling in freshwater sediments: a cryptic driving force of iron deposition and phosphorus mobilization. Sci Total Environ 657:1294–1303
Xu D, Chen YF, Ding SM, Sun Q, Wang Y, Zhang CS (2013) Diffusive gradients in thin films technique equipped with a mixed binding gel for simultaneous measurements of dissolved reactive phosphorus and dissolved iron. Environ Sci Technol 47:10477–10484

Yang X, Lu X (2014) Drastic change in China's lakes and reservoirs over the past decades. Sci Rep 4:6041

Yang CH, Yang P, Geng J, Yin HB, Chen KN (2020) Sediment internal nutrient loading in the most polluted area of a shallow eutrophic lake (Lake Chaohu, China) and its contribution to lake eutrophication. Environ Pollut 262:114292

Yin H, Yang P, Kong M, Li W (2020) Preparation of the lanthanum–aluminum-amended attapulgite composite as a novel inactivation material to immobilize phosphorus in lake sediment. Environ Sci Technol 54:11602–11610

Yu J, Ding S, Zhong J, Fan C, Chen Q, Yin H, Zhang L, Zhang Y (2017) Evaluation of simulated dredging to control internal phosphorus release from sediments: focused on phosphorus transfer and resupply across the sediment-water interface. Sci Total Environ 592:662–673

Zhang HG, Lyu T, Bi L, Hamilton GT, Pan G (2018) Combating hypoxia/anoxia at sediment-water interfaces: a preliminary study of oxygen nanobubble modified clay materials. Sci Total Environ 637–638:550–560

Zhao Y, Yang Z, Xia X, Wang F (2012) A shallow lake remediation regime with *Phragmites australis*: incorporating nutrient removal and water evapotranspiration. Water Res 46:5635–5644